

DUPS

NAVAL POSTGRADUATE SCHOOL Monterey, California

AD-A257 326



DTIC
ELECTE
NOV 23 1992
S C D

THESIS

**EFFECTS OF INTERFACIAL DEBONDING AND FIBER
BREAKAGE ON STATIC AND DYNAMIC BUCKLING OF
FIBERS EMBEDDED IN MATRICES**

by

Metin Serttunc

September, 1992

Thesis Advisor:

Young W. Kwon

Approved for public release; distribution is unlimited

**BEST
AVAILABLE COPY**

92 11 20 002

92-29894

Dup

REPORT DOCUMENTATION PAGE				
1a. REPORT SECURITY CLASSIFICATION Unclassified		1b. RESTRICTIVE MARKINGS		
2a. SECURITY CLASSIFICATION AUTHORITY		3. DISTRIBUTION/AVAILABILITY OF REPORT Approved for public release; distribution is unlimited.		
2b. DECLASSIFICATION/DOWNGRADING SCHEDULE				
4. PERFORMING ORGANIZATION REPORT NUMBER(S)		5. MONITORING ORGANIZATION REPORT NUMBER(S)		
6a. NAME OF PERFORMING ORGANIZATION Naval Postgraduate School	6b. OFFICE SYMBOL (If applicable) ME	7a. NAME OF MONITORING ORGANIZATION Naval Postgraduate School		
6c. ADDRESS (City, State, and ZIP Code) Monterey, CA 93943-5000		7b. ADDRESS (City, State, and ZIP Code) Monterey, CA 93943-5000		
8a. NAME OF FUNDING/SPONSORING ORGANIZATION	8b. OFFICE SYMBOL (If applicable)	9. PROCUREMENT INSTRUMENT IDENTIFICATION NUMBER		
8c. ADDRESS (City, State, and ZIP Code)		10. SOURCE OF FUNDING NUMBERS		
		Program Element No.	Project No.	Task No.
11. TITLE (Include Security Classification) EFFECTS OF INTERFACIAL DEBONDING AND FIBER BREAKAGE ON STATIC AND DYNAMIC BUCKLING OF FIBERS EMBEDDED IN MATRICES				
12. PERSONAL AUTHOR(S) METIN SERTTUNC				
13a. TYPE OF REPORT Master's Thesis	13b. TIME COVERED From To	14. DATE OF REPORT (year, month, day) SEPTEMBER 1992	15. PAGE COUNT 45	
16. SUPPLEMENTARY NOTATION The views expressed in this thesis are those of the author and do not reflect the official policy or position of the Department of Defense or the U.S. Government.				
17. COSATI CODES		18. SUBJECT TERMS (continue on reverse if necessary and identify by block number) buckling of composites		
FIELD	GROUP			SUBGROUP
19. ABSTRACT (continue on reverse if necessary and identify by block number) Analyses were performed for static and dynamic buckling of a continuous fiber embedded in a matrix and fiber breakage in order to determine the effects of interfacial debonding on the critical buckling load and the domain of instability. A beam on elastic foundation model was used for this study. The study showed that a local interfacial debonding between a fiber and a surrounding matrix resulted in an increase of the wavelength of the buckling mode. An increase of the wavelength yielded a decrease of the static buckling load and lowered the dynamic instability domain. In general, the effect of a partial or complete interfacial debonding was more significant on the domain of dynamic instability than on the effects of static buckling load. For dynamic buckling of a fiber, a local debonding of size 10 to 20 percent of the fiber length had the most important influence on the domains of dynamic instability regardless of the location of debonding and the boundary conditions of the fiber. For static buckling, the location of a local debonding was critical to a free-simply supported fiber but not to a fiber with both ends simply supported. Fiber breakage also lowered the critical buckling load significantly.				
20. DISTRIBUTION/AVAILABILITY OF ABSTRACT <input checked="" type="checkbox"/> UNCLASSIFIED/UNLIMITED <input type="checkbox"/> SAME AS REPORT <input type="checkbox"/> DTIC USERS		21. ABSTRACT SECURITY CLASSIFICATION Unclassified		
22a. NAME OF RESPONSIBLE INDIVIDUAL Young W. Kwon		22b. TELEPHONE (Include Area code) (408) 646-3385	22c. OFFICE SYMBOL ME/kw	

Approved for public release; distribution is unlimited.

**Effects of Interfacial Debonding and Fiber Breakage
on Static and Dynamic Buckling of Fibers in Matrices**

by

Metin Serttunc

**Lieutenant (j.g.), Turkish Navy
B.S.M.E., Dz. H. O. Turkey. 1986**

Submitted in partial fulfillment
of the requirements for the degree of

MASTER OF SCIENCE IN MECHANICAL ENGINEERING

from the

**NAVAL POSTGRADUATE SCHOOL
SEPTEMBER 1992**

Author:



Metin Serttunc

Approved by:



Young W. Kwon, Thesis Advisor



**Matthew D. Kelleher, Chairman
Department of Mechanical Engineering**

ABSTRACT

Analyses were performed for static and dynamic buckling of a continuous fiber embedded in a matrix in order to determine the effects of interfacial debonding and fiber breakage on the critical buckling load and the domain of instability. A beam on elastic foundation model was used for the study. The study showed that a local interfacial debonding between a fiber and a surrounding matrix resulted in an increase of the wavelength of the buckling mode. An increase of the wave length yielded a decrease of the static buckling load and lowered the dynamic instability domain.

In general, the effect of a partial or complete interfacial debonding was more significant on the domain of dynamic instability than on the effects of static buckling load. For dynamic buckling of a fiber, a local debonding of size 10 to 20 percent of the fiber length had the most important influence on the domains of dynamic instability regardless of the location of debonding and the boundary conditions of the fiber. For static buckling, the location of a local debonding was critical to a free-simply supported fiber but not to a fiber with both ends simply supported. Fiber breakage also lowered the critical buckling load significantly.

DTIC QUALITY INSPECTED 4

Accession For	
NTIS SERIAL	<input checked="" type="checkbox"/>
DTIC TAB	<input type="checkbox"/>
Unannounced	<input type="checkbox"/>
Justification	
By	
Distribution/	
Availability Codes	
Avail and/or	
Dist	Special
A-1	

TABLE OF CONTENTS

I. INTRODUCTION	1
II. ANALYSIS AND MODELING	5
A. NUMERICAL ANALYSIS	5
B. NUMERICAL MODELLING	10
III. RESULTS AND DISCUSSIONS	14
A. STATIC BUCKLING	14
B. DYNAMIC BUCKLING	22
IV. CONCLUSIONS	34
LIST OF REFERENCES	36
INITIAL DISTRIBUTION LIST	38

Duplicated

ACKNOWLEDGEMENTS

I would like to express my sincere thanks and gratitude to Dr. Young W. Kwon for his guidance, encouragement, and support throughout this research. For technical support and patience I thank all the other instructors in Mechanical Engineering departement.

I. INTRODUCTION

Buckling is one of the important failure modes of structures subjected to compressive inplane loads. Buckling in a continuous fibrous composite panel may include global buckling of the panel as well as buckling of fibers embedded in a surrounding matrix. Fiber buckling is one of the major causes of reduced compressive strength of a composite panel. As a result, the compressive strength of a composite is generally lower than its tensile strength.

Some of the initial studies on fiber buckling were given in references (Dow and Gruntfest 1960, Fried and Kaminetsky 1964, Leventz 1964, and Rosen 1965). These studies found that fiber buckling was an important cause in reducing the compressive strength of composites. Rosen (1965) investigated the fiber buckling using an energy method. He considered two-dimensional arrays of fibers embedded in a matrix material, and computed critical fiber buckling loads for two different modes of buckling: the shear mode and the extension mode. In the shear mode, two neighboring fibers buckle in phase. On the other hand, two neighboring fibers buckle out of phase in the extension mode. Of the two fiber buckling modes, the one which results in a lower critical buckling load governs the buckling mode.

Experimental studies were performed to investigate fiber buckling within a supporting matrix material (Lager and June 1969, and Dale and Baer 1974). The experimental results agreed with Rosen's predictions. For a very low fiber volume fraction, the extension mode predominated, while the shear mode predominates for composites with fiber volume fractions of interest in practical application. A postbuckling study of fibers was performed by Maewal (1981). He found that the effect of initial geometric imperfections like initial waviness of fibers on the microbuckling stress was not significant.

Experimental studies showed that compression failure in straight fiber laminated test specimens initiated at a free edge (Hahn and Williams 1984). In order to enhance the understanding of the effect of the free edge on the initiation of the buckling process, a study of fiber buckling was undertaken by Wass, Babcock, and Knauss (1989). They used a model of a beam supported by an elastic matrix. They concluded that, for low fiber volume fractions, the critical strain values at a free edge were lower than the predictions using Rosen's model. For high volume fractions, however, they found the beam model was not valid for the purpose of their study.

All the studies mentioned above assumed perfect bonding between a fiber and its surrounding matrix. Lanir and Fung (1972) studied the effect of interfacial separation on fiber buckling. They calculated deflections of the postbuckled

wave-like shape of fibers. They also stated that the critical buckling load of a fiber was the same as that of a free column in case of interfacial separation between the fiber and matrix. This was the situation where a surrounding matrix did not affect the fiber buckling due to separation. However, if there is an interfacial separation between a fiber and a surrounding matrix but they are in interfacial contact without pressing each other before buckling, the matrix material still supports the fiber after the buckling occurs as shown in Figure 1. In a buckled position, the compressed matrix side (the bottom side in Figure 1) provides reactions to a fiber.

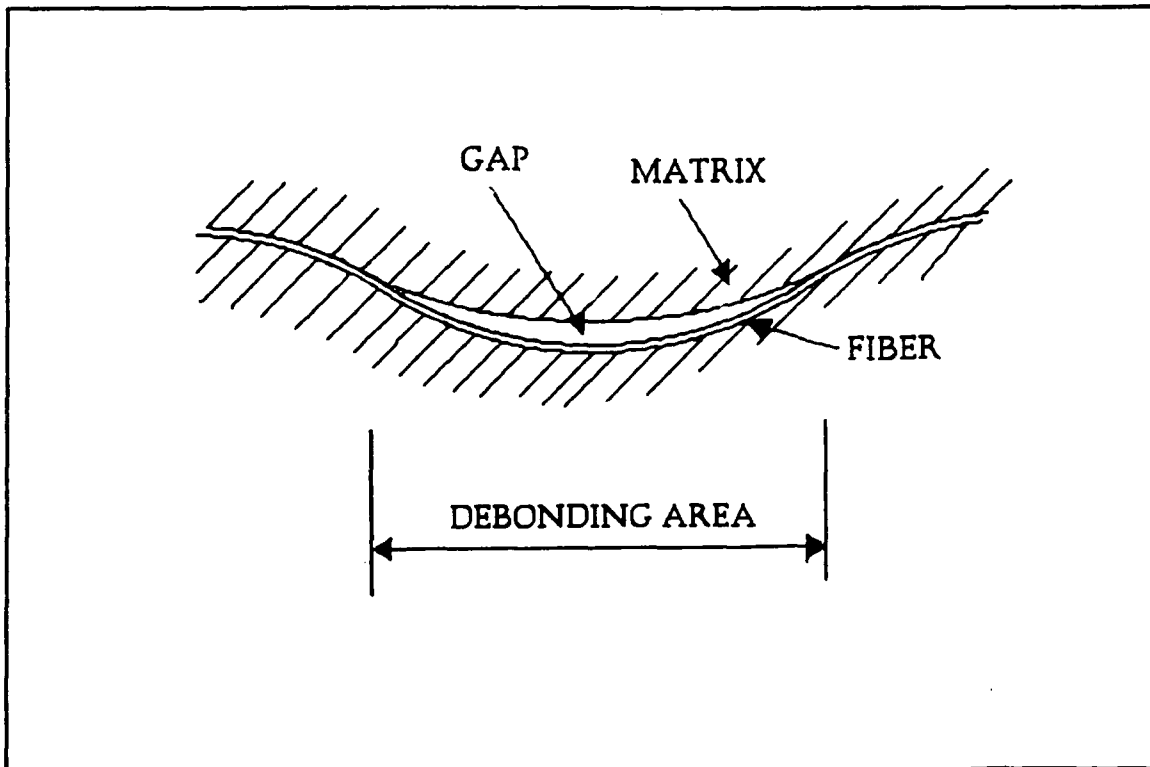


Figure 1. Interfacial debonding between a fiber and a supporting matrix after fiber buckling.

The present thesis computes critical buckling loads of fibers with partial interfacial debonding from surrounding matrices using the finite element method. The buckling loads with debonding are compared to the buckling loads without debonding for various fibrous materials. Different locations and magnitudes of partial debonding are considered to investigate their effects on the critical buckling load. The study includes not only static buckling but also dynamic buckling of a fiber embedded in a matrix material. Furthermore, the effect of fiber breakage on the fiber buckling is also investigated.

II. ANALYSIS AND MODELING

A. NUMERICAL ANALYSIS

A beam on elastic foundation model was used for this study. The Bernoulli-Navier beam theory was used to model a fiber, and a surrounding matrix was modeled as an elastic foundation. The spring constant of an elastic foundation was computed from the expression developed by Herrmann, Mason and Chan (1965). The spring constant is given below:

$$k = \frac{8\pi G_m (1 - \nu_m)}{(3 - 4\nu_m) K_0(2\pi r/\delta) + (\pi r/\delta) K_1(2\pi r/\delta)} \quad (1)$$

in which

k = spring constant of the elastic foundation,

G = shear modulus,

ν = Poisson's ratio,

r = radius of the fiber,

δ = wavelength of the deformed fiber (see Figure 2),

K_0 = zeroth-order modified Bessel function of the second kind,

K_1 = first-order modified Bessel function of the second kind,

and the subscript m denotes the matrix. The spring constant in Equation (1) was obtained assuming that the moment foundation modulus associated with the beam rotation was negligible. This

assumption is valid when the shear modulus of a fiber is much larger than that of a matrix.

The equation of beam bending is:

$$m \frac{\partial^2 w}{\partial t^2} + E_f I_f \frac{\partial^4 w}{\partial x^4} - P \frac{\partial^2 w}{\partial x^2} + kw = 0 \quad (2)$$

where

m = mass of the fiber per unit length,

w = transverse deflection of the fiber,

E = elastic modulus,

I = moment inertia of cross-section,

P = axial load applied to the fiber (a positive value denotes a compressive force), and

x direction is along the fiber axis while t and f denote time and fiber respectively. Applying the method of weighted residual along with the weak formulation to equation (2) gives;

$$\int_0^L m \bar{w} w_{,tt} dx + \int_0^L E_f I_f \bar{w}_{,xx} w_{,xx} dx - \int_0^L P \bar{w}_{,x} w_{,x} dx + \int_0^L k \bar{w} w dx + [E_f I_f w_{,xxx} \bar{w}] \Big|_0^L - [E_f I_f w_{,xx} \bar{w}_{,x}] \Big|_0^L = 0. \quad (3)$$

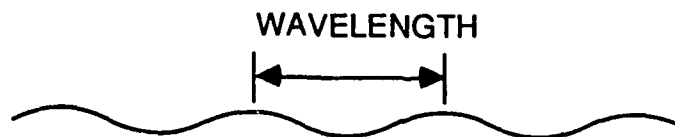


Figure 2. Wavelength of a buckled fiber

In this equation, $w_{,x}$ indicates a partial derivative of w with respect to x , \bar{w} is a test function. This equation contains second derivatives so that it is needed to assume an interpolation function for w that has both continuous deflection, w , and continuous slope, w' , between elements. One common choice is the cubic Hermitian polynomial presented in below.

$$\begin{aligned}
 H_1(r) &= 2r^3 - 3r^2 + 1 \\
 H_2(r) &= (r^3 - 2r^2 + r)h \\
 H_3(r) &= 3r^2 - 2r \\
 H_4(r) &= (r^3 - r^2)h
 \end{aligned}
 \tag{4}$$

where $r=x/h$ and h represents the length of element. Their derivatives with respect to x are

$$\begin{aligned}
 H_1' &= (6r^2 - 6r) / h & H_1'' &= (12r - 6) / h^2 \\
 H_2' &= 3r^2 - 4r + 1 & H_2'' &= (6r - 4) / h \\
 H_3' &= (6r - 6r^2) / h & H_3'' &= (6 - 12r) / h^2 \\
 H_4' &= 3r^2 - 2r & H_4'' &= (6r - 2) / h
 \end{aligned}
 \tag{5}$$

where prime, ', denotes a derivative

Substituting the Hermitian shape function to Equation (3) after discretization of the domain into a number of finite elements results in:

$$\int_h m [H]^T [H] dx + \int_h E_f I_f [H'']^T [H''] dx - \int_h P [H']^T [H'] dx + \int_h k [H]^T [H] dx = 0
 \tag{6}$$

or

$$[M]\{\ddot{w}\} + [K_{EI}]\{w\} - [K_p]\{w\} + [K_K]\{w\} = 0 . \quad (7)$$

The superimposed dot denotes temporal derivatives. The details of matrices in Equation (7) are given below:

$$[K_{EI}] = \frac{EI}{h^4} \int_0^h \begin{bmatrix} H_1''H_1'' & H_1''H_2'' & H_1''H_3'' & H_1''H_4'' \\ H_2''H_1'' & H_2''H_2'' & H_2''H_3'' & H_2''H_4'' \\ H_3''H_1'' & H_3''H_2'' & H_3''H_3'' & H_3''H_4'' \\ H_4''H_1'' & H_4''H_2'' & H_4''H_3'' & H_4''H_4'' \end{bmatrix} dx$$

$$= \frac{EI}{h^3} \begin{bmatrix} 12 & 6h & -12 & 6h \\ 6h & 4h^2 & -6h & 2h^2 \\ -12 & -6h & 12 & -6h \\ 6h & 2h^2 & -6h & 4h^2 \end{bmatrix} \quad (8)$$

$$[K_K] = \int_0^h k \begin{bmatrix} H_1H_1 & H_1H_2 & H_1H_3 & H_1H_4 \\ H_2H_1 & H_2H_2 & H_2H_3 & H_2H_4 \\ H_3H_1 & H_3H_2 & H_3H_3 & H_3H_4 \\ H_4H_1 & H_4H_2 & H_4H_3 & H_4H_4 \end{bmatrix} dx$$

$$= \frac{k}{420} \begin{bmatrix} 156 & 22h & 54 & -13h \\ 22h & 4h^2 & 13h & -3h^2 \\ 54 & 13h & 156 & -22h \\ -13h & -3h^2 & -22h & 4h^2 \end{bmatrix} \quad (9)$$

$$[K_p] = \frac{P}{h^2} \int_0^h \begin{bmatrix} H_1'H_1' & H_1'H_2' & H_1'H_3' & H_1'H_4' \\ H_2'H_1' & H_2'H_2' & H_2'H_3' & H_2'H_4' \\ H_3'H_1' & H_3'H_2' & H_3'H_3' & H_3'H_4' \\ H_4'H_1' & H_4'H_2' & H_4'H_3' & H_4'H_4' \end{bmatrix} dx$$

$$= \frac{P}{30h} \begin{bmatrix} 36 & 3h & -36 & 3h \\ 3h & 4h^2 & -3h & -h^2 \\ -36 & -3h & 36 & -3h \\ 3h & -h^2 & -3h & 4h^2 \end{bmatrix} \quad (10)$$

$$[M] = m \int_0^h \begin{bmatrix} H_1H_1 & H_1H_2 & H_1H_3 & H_1H_4 \\ H_2H_1 & H_2H_2 & H_2H_3 & H_2H_4 \\ H_3H_1 & H_3H_2 & H_3H_3 & H_3H_4 \\ H_4H_1 & H_4H_2 & H_4H_3 & H_4H_4 \end{bmatrix} dx$$

$$= \frac{m}{420} \begin{bmatrix} 156 & 22h & 54 & -13h \\ 22h & 4h^2 & 13h & -3h^2 \\ 54 & -13h & 156 & -22h \\ -13h & -3h^2 & -22h & 4h^2 \end{bmatrix} \quad (11)$$

In the present study, the diagonal mass matrix was also used in addition to the consistent mass matrix given equation (11).

The diagonal mass matrix is

$$[M] = \frac{m}{78} \begin{bmatrix} 39 & 0 & 0 & 0 \\ 0 & h^2 & 0 & 0 \\ 0 & 0 & 39 & 0 \\ 0 & 0 & 0 & h^2 \end{bmatrix} \quad (12)$$

For the static buckling analysis, the mass term in Equation (3) drops out, and the resultant equation becomes an eigenvalue problem as given below:

$$\det [[K_{EI}] + [K_K] - P_{cr} [K_P]] = 0 \quad (13)$$

where P_{cr} is the critical buckling load. A compressive load was assumed to be positive. The elastic foundation increases the critical buckling load significantly compared to the case of a beam without any foundation support. Furthermore, mode

shapes of buckling become complicated due to the elastic foundation (see Timoshenko and Gere 1961, and Hetenyi 1974). For example, the mode shape for the smallest critical buckling load is dependent on the geometric and material properties of the beam and foundation. The mode shape is unknown a priori.

In order to determine the spring constant from Equation (1), the wavelength must be known. However, the wavelength is unknown because the mode shape is unknown a priori. Therefore, an iteration process is necessary to find the correct wavelength of the buckled beam. The flowchart for the iteration procedure is given in Figure 3.

B. NUMERICAL MODELLING

Interfacial debonding between a fiber and the supporting matrix is modeled as explained below. It is assumed that there is no gap at the interface between the fiber and the matrix even if there is debonding at the interface. As a result, if a fiber buckles at the debonded interface, the compressed side of a matrix material still supports the fiber while the other side of the matrix does not provide any support as shown in Figure 1. If there is an enough friction to prevent sliding at a debonded interface which is located at the compressed side of a matrix, the interface under compression behaves just like a bonded interface. A fully bonded matrix along the circumference of a buckled fiber supports the fiber at both the compressed and elongated sides of the matrix, while a

matrix debonded along the circumference of a buckled fiber supports the fiber only at the compressed side of the matrix. Therefore, it is reasonable to assume that the matrix at a debonded interface provides half of the support of a perfectly bonded matrix if a correct wavelength is obtained at the debonded interface. However, the wavelength changes with the debonding. As a result, an iteration is required to determine the correct wavelength and the spring constant at a debonded interface.

The fiber breakage is modeled in the following way. Once there is a fiber breakage, there is no continuity of the slope of the deflection at the broken position. However, the lateral deflection is assumed to be continuous. Otherwise, there is no axial force to balance the two broken fibers in the axial direction since the spring does not constrain the axial motion. Debonding is also assumed to occur from the broken position.

For the study of dynamic instability, the axial force in Equation (3) is assumed to be a harmonic function. That is,

$$P = p \cos(\theta t) \quad (14)$$

where p is the magnitude of the pulsating inplane force and θ is the circular frequency of the pulsation. Let the transverse displacement vector be expressed in terms of trigonometric forms;

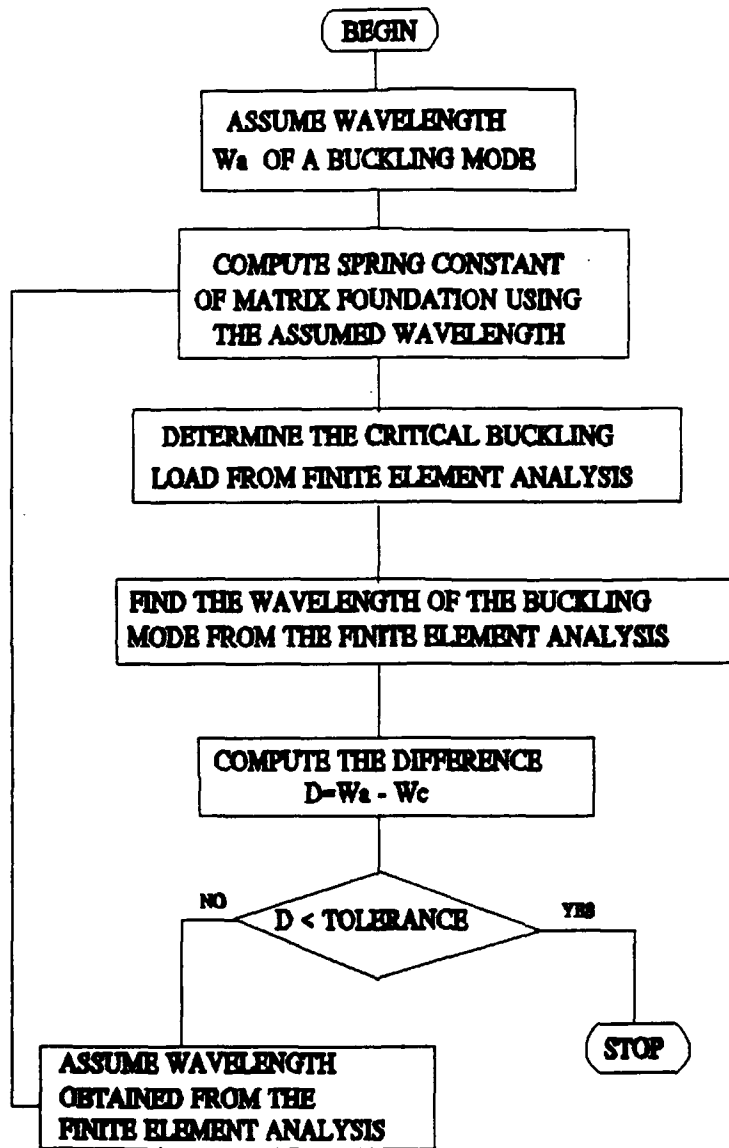


Figure 3. An iteration procedure to find the wavelength of the buckled shape.

$$\{w\} = \sum_{i=1,3,\dots}^{\infty} \{\ddot{u}_i\} \sin \frac{i\theta t}{2} + \sum_i \{\bar{u}_i\} \cos \frac{i\theta t}{2} \quad (15)$$

where \ddot{u} and \bar{u} are time independent vectors of the nodal transverse displacement. Substituting Equations (14) and (15) into Equation (7), and considering the first term (i.e. $i=1$) of Equation (15) as the first-order approximation yields the following eigenvalue matrix equation:

$$\det \left[[K_{EI}] + [K_R] \pm \frac{b}{2} [K_P] - \frac{\theta^2}{4} [M] \right] = 0 \quad (16)$$

The eigenvalues of θ obtained from Equation (16) determine the boundary of domain of principal instability. For the mass matrix in Equation (16), both diagonal and consistent mass matrices are used for comparison. The transverse shear effect and rotatory inertia effect are neglected in this study because the length of the fiber under consideration is much larger than the cross-sectional dimension. A previous study of dynamic instability of layered composite plates (Kwon 1991) showed that the transverse shear effect was found to be negligible if the length of a plate was much larger than a plate thickness.

III. RESULTS AND DISCUSSIONS

A. STATIC BUCKLING

Under consideration in this study were fibers made of graphite, Kevlar, and glass embedded in epoxy, and boron embedded in an aluminum. Their material properties were different so that the effect of different materials on buckling was studied. The material properties are tabulated in Table 1, which were obtained from a textbook (Tsai and Hahn 1980).

TABLE I. MATERIAL PROPERTIES OF FIBERS AND MATRICES

MATERIAL	ELASTIC MODULUS (GPa)	DENSITY (g/cm ³)
GRAPHITE	230	1.75
KEVLAR	120	1.44
GLASS	72	2.6
BORON	410	2.6
EPOXY	3.9	
ALUMINUM	70	

The first study considered a fiber of dimension $L/r = 100$ embedded in an epoxy. Here L/r is the ratio of the beam length to radius. Both ends were assumed to be simply supported. Interfacial debonding was assumed to occur at the center of

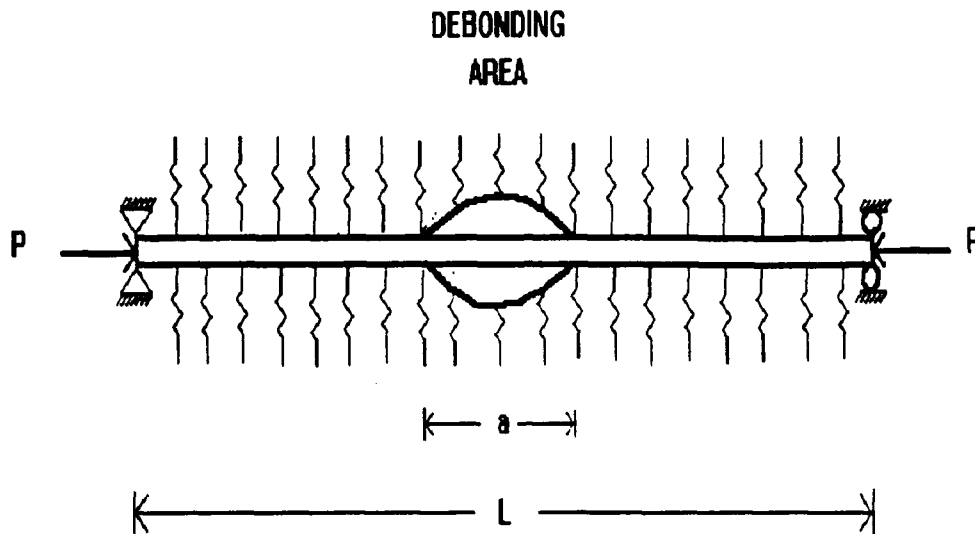


Figure 4. A simply supported fiber with interfacial debonding at the center.

the fiber as shown in Figure 4. The effect of the interfacial debonding on the static buckling load is shown in Figure 5 for four different cases. The results revealed that the percentage reduction in the critical buckling load was almost independent of the elastic moduli of the fibers even if the absolute magnitude of the buckling loads varied for the three different fibers. The graphite fiber had the largest magnitude of buckling load and the glass fiber had the smallest buckling load because of their elastic moduli. There was approximately a 35 percent decrease of the static buckling load due to complete debonding. In the case of the boron fiber embedded in an aluminum matrix, there was a 42 percent decrease in the

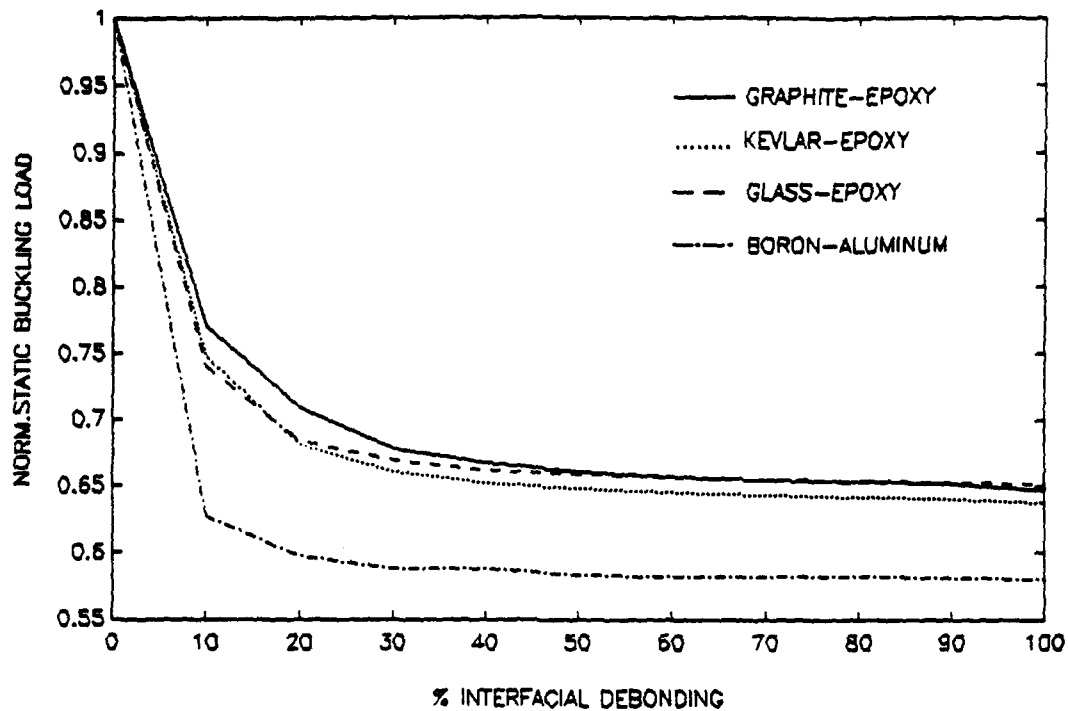


Figure 5. Effect of interfacial debonding on the buckling load for simply supported fibers.

static buckling load due to complete debonding. For all cases, it can be seen that, the reduction of the buckling load was significant for initial 10 to 20 percent of debonding area and changed very gradually after that.

The static buckling mode shapes varied as the interfacial debonding increased. The shape changed from a symmetrical mode to an antisymmetrical mode or vice versa as the debonding progressed. In addition, the wavelength changed with the debonding. Figure 6 shows buckled shapes of the Kevlar fiber for different debonding sizes. The wavelength at the debonded area was larger than that at the bonded area. The relative magnitude of the buckled shape was much larger at the debonded

area than at the bonded area if there was a partial debonding through the length of the fiber. Therefore, even if there is waviness at the bonded area in Figure 6(b), it is not reflected in the buckled shape. The graphite fiber had the largest wavelength while the glass fiber had the smallest wavelength in an epoxy matrix.

In order to examine the effect of fiber length on buckling, a fiber with ratio $L/r = 200$ was studied. The absolute magnitude of critical load decreased for a fiber of $L/r = 200$ when compared to that of a fiber of $L/r = 100$, but the percentage reduction of the critical loads caused by the interfacial debonding remained almost the same for the two fibers of different lengths. The wavelength was larger for the longer fiber. The location of partial debonding was varied to investigate its effect on the buckling load. For a fiber simply supported at both ends, the location of debonding did not make much difference on the decrease of buckling load. An initial debonding at any location was the most critical factor in reducing the critical buckling load.

The next study was to determine the effect of different boundary conditions. A fiber with one end simply supported and the other end free was considered. As before three different fibrous materials were studied. First, a partial debonding was assumed to start from the free end as shown in Figure 7. Figure 8 shows the reduction of the critical buckling load as a result of increased partial debonding. An initial debonding



(a) Perfect interfacial bonding

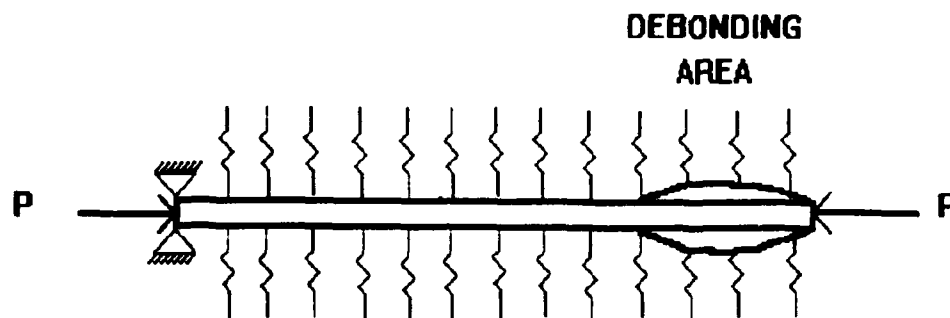


(b) 50 % interfacial debonding at the center

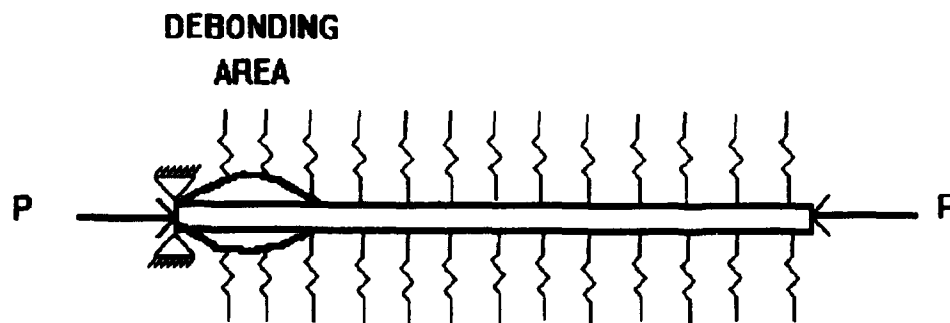


(c) complete interfacial debonding

Figure 6. Buckling modes of Kevlar fiber.



(a) Debonding starting from free end



(b) Debonding starting from simply supported end

Figure 7. A free simply supported fiber with different locations of interfacial debonding.

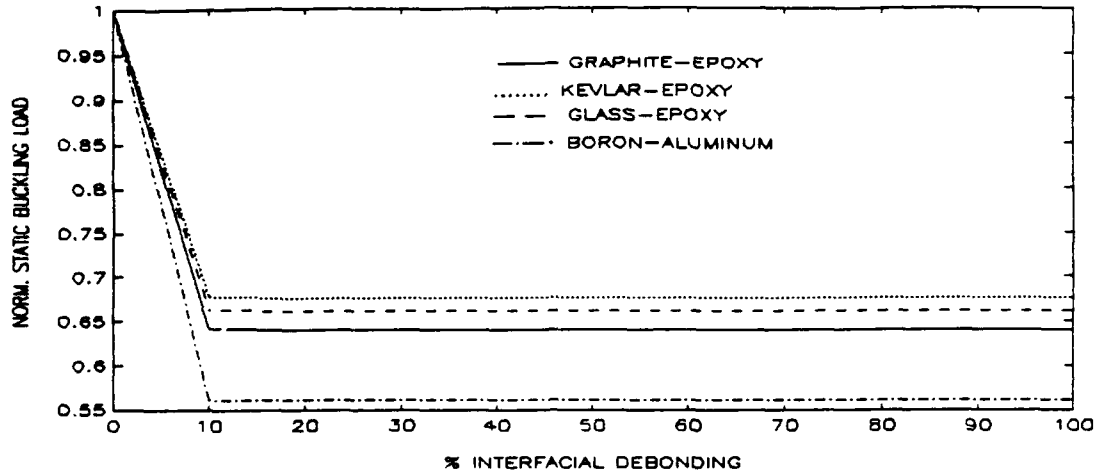


Figure 8. Effect of interfacial debonding on the buckling load for free simply supported fibers. (Debonding starts from free end)

of 10 percent decreased the buckling load significantly while no further debonding affected the buckling load. When a partial debonding started at the simply supported end as shown in Figure 7, there was no change in the buckling load until there was at least 10 percent debonding as shown in Figure 9. That is, the location was very critical in decreasing the buckling load. This result was contrary to that for a fiber with both ends simply supported.

The last study for static buckling was to examine the effect of fiber breakage along with interfacial debonding. A fiber with simply supported ends was considered. As before four different fiber materials were used. After a fiber breakage, partial debonding was assumed to start from that point. (See Figure 10) Figure 11 shows a comparison of the

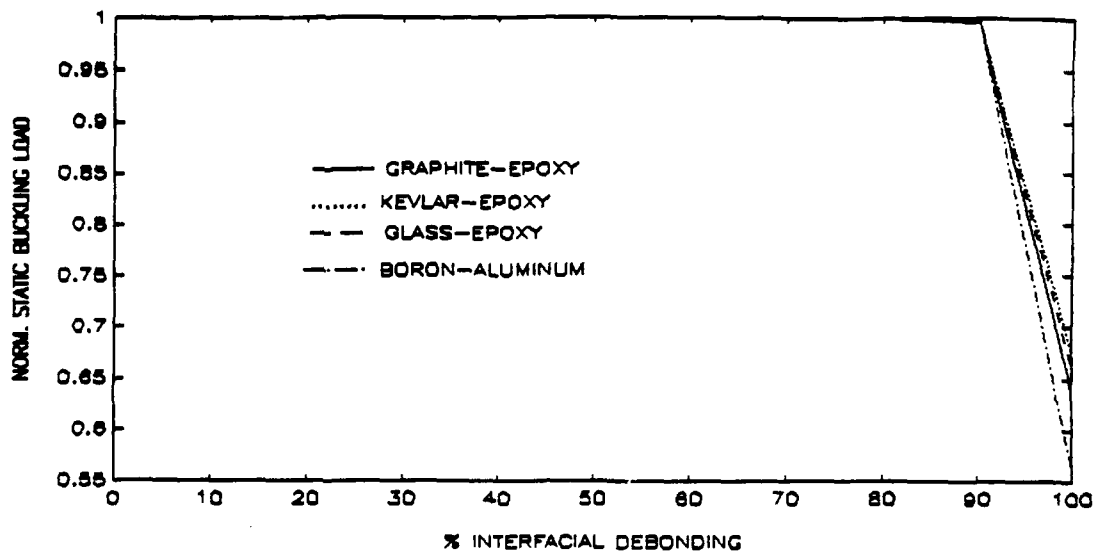


Figure 9. Effect of interfacial debonding on the buckling load for free-simply supported fibers. (Debonding starts from the supported end)

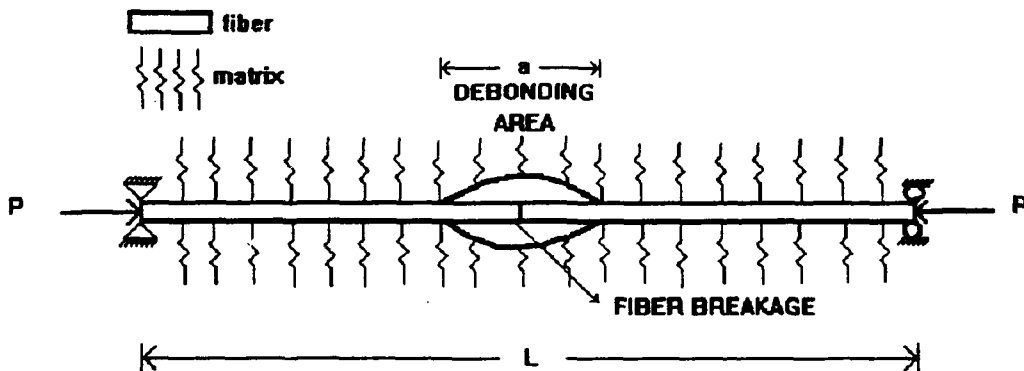


Figure 10. Fiber breakage along with interfacial debonding.

fibers with a breakage and without it. A fiber breakage showed a 50 percent decrease of the critical load, independent of fiber breakage locations except for very close distances from the supports. Fiber breakage near the supports is more

critical. Debonding effects after a fiber breakage were very similar to the case without fiber breakage. An initial 10 percent debonding decreased the buckling load significantly and after 30 percent no further debonding changed the buckling load.

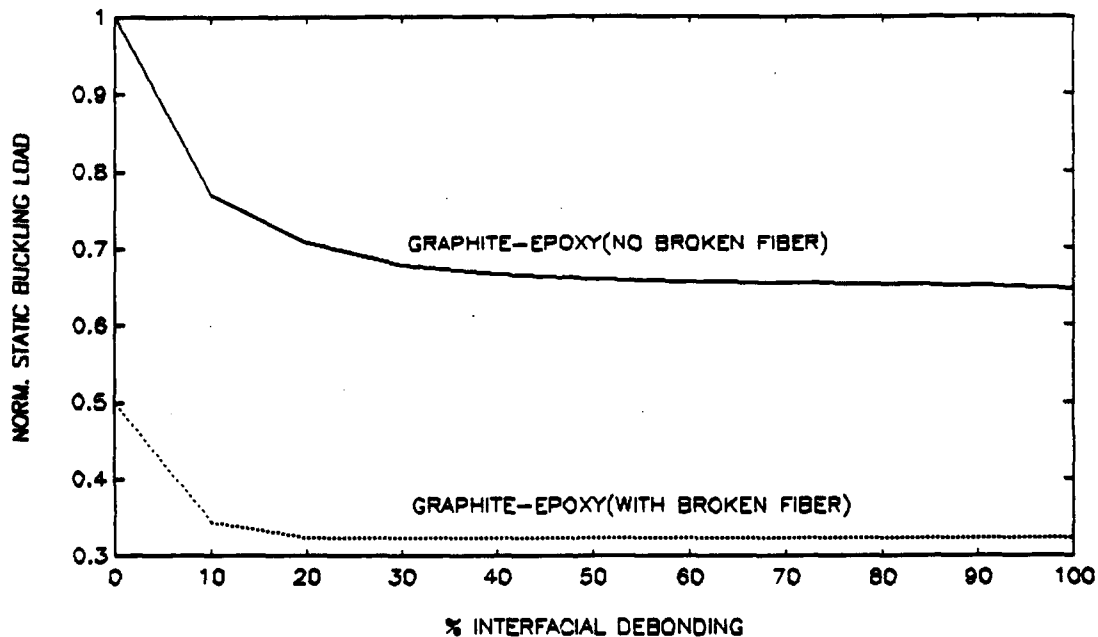


Figure 11. Comparison of critical buckling loads for a broken fiber and a fiber without breakage.

B. DYNAMIC BUCKLING

The domains of dynamic instability were plotted in Figures 12-15 for four different cases (Graphite-epoxy, Kevlar-epoxy, Glass-epoxy and Boron-aluminum). Each different case has $L/r=100$ ratio with simply supported ends. The axial force and

circular frequency in all figures were normalized as shown below:

$$P_{\text{NORM}} = \frac{p}{P_{\text{CR}}} \quad (17)$$

$$\theta_{\text{NORM}} = \frac{\theta}{2\Omega} \quad (18)$$

where P_{CR} is a static buckling load and Ω is the natural frequency. A local debonding was assumed to begin from the center. An interfacial debonding lowered the instability domains. The results showed that the instability domains of fibers embedded in an epoxy matrix were lowered 35 percent at full debonding compared with no debonding. The instability domain of boron-aluminum was lowered by 42 percent for the same comparison. An initial 10 to 20 percent local debonding influenced the instability domains significantly but a further increase of debonding size had very little affect. Local debonding also widened the instability domains. Although the instability domains between 10 percent debonding and 100 percent debonding were not shown in Figure 12, these instability domains were calculated and were located between the outer borders of the mentioned domains.

After calculating the elastic moduli ratios, which was shown in Table 2, it was seen that, when the elastic moduli ratio decreased, the instability domains between 10 percent debonding and full debonding scattered over a smaller area.

TABLE II. ELASTIC MODULI RATIOS BETWEEN FIBERS AND MATRICES

FIBER-MATRIX	ELASTIC MODULI RATIO
GRAPHITE-EPOXY	58.97
KEVLAR-EPOY	30.77
GLASS-EPOXY	18.46
BORON-ALUMINUM	5.86

When a local debonding started at both simply supported ends, the debonding effect was less critical than a local debonding starting at the center until it progressed 20 percent debonding. For a debonding size larger than 20 percent of the beam, the debonding effect was not sensitive to the location (see Figures 16-19).

Fibers with free-simply supported ends were also studied for dynamic buckling. Figures 20 through 27 show the change of domains of instability caused by an interfacial debonding. Figures 20 through 23 represent the case of a debonding starting from the free end while Figures 24 through 27 represent the case a debonding starting from the simply supported end. The debonding starting from the free end was more critical to the instability domains than that starting from the supported end. However, the dynamic buckling was less sensitive to the location of a debonding than the static buckling for free-simply supported fibers. The size of a

debonding was more important than location in influencing the instability domain.

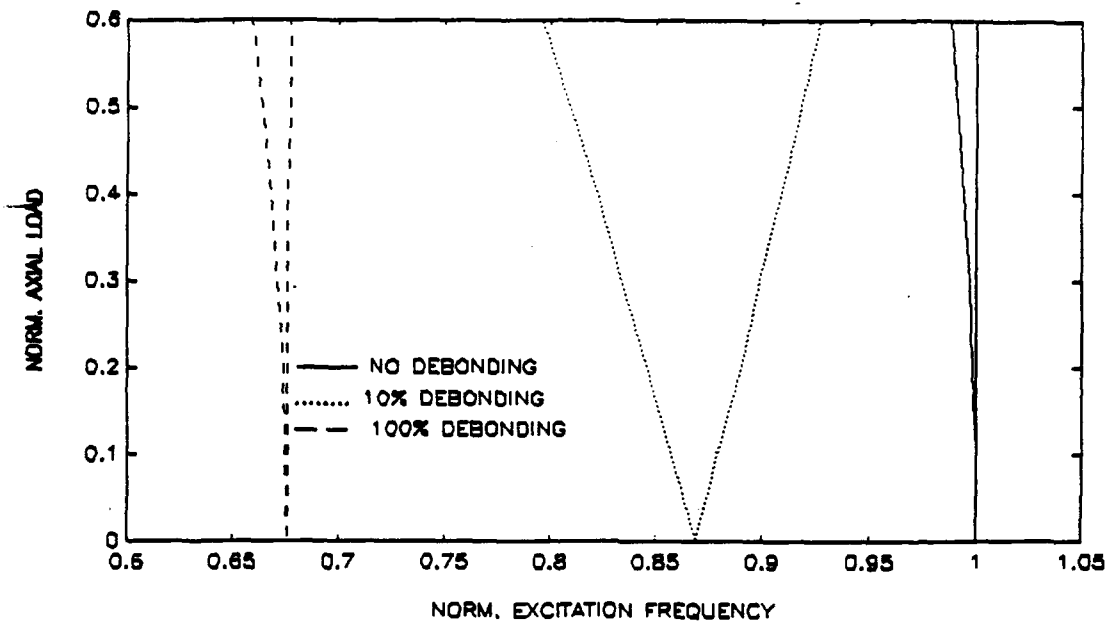


Figure 12. Instability domains Kevlar-epoxy with free and simply supported ends (Debonding started from the simply supported end).

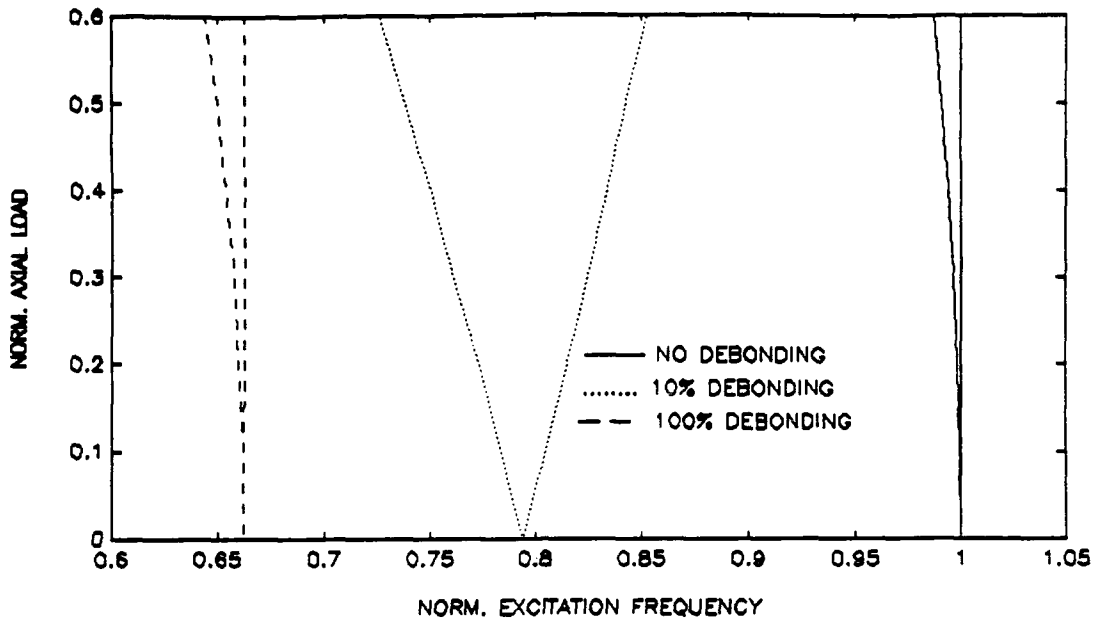


Figure 13. Instability domains glass-epoxy with free and simply supported ends (Debonding started from the simply supported end).

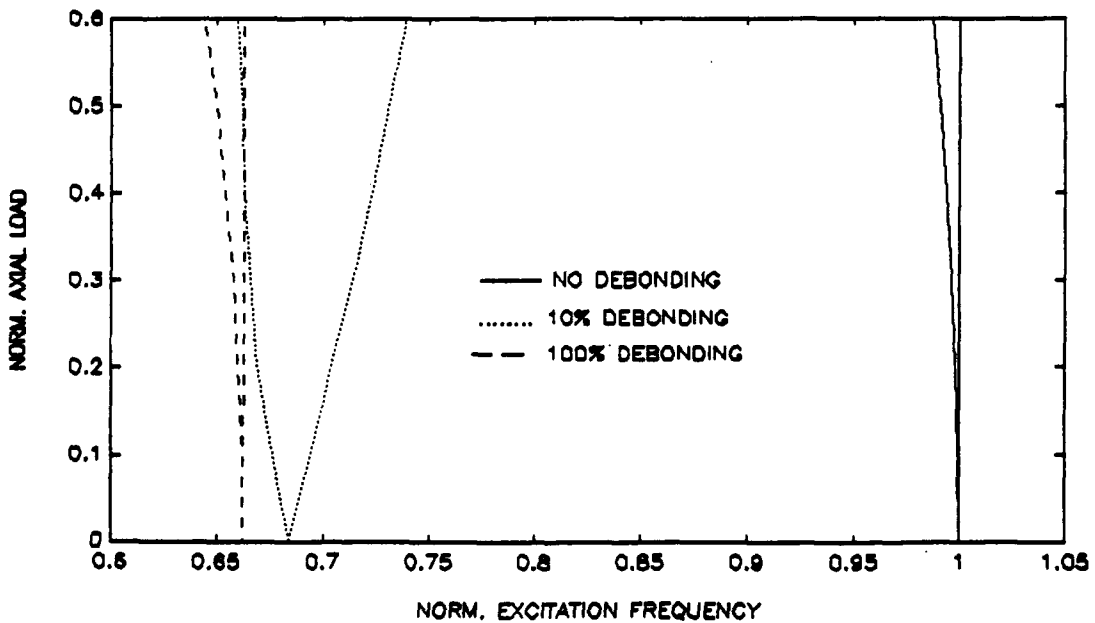


Figure 14. Instability domains glass-epoxy with free and simply supported ends (Debonding started from the free end).

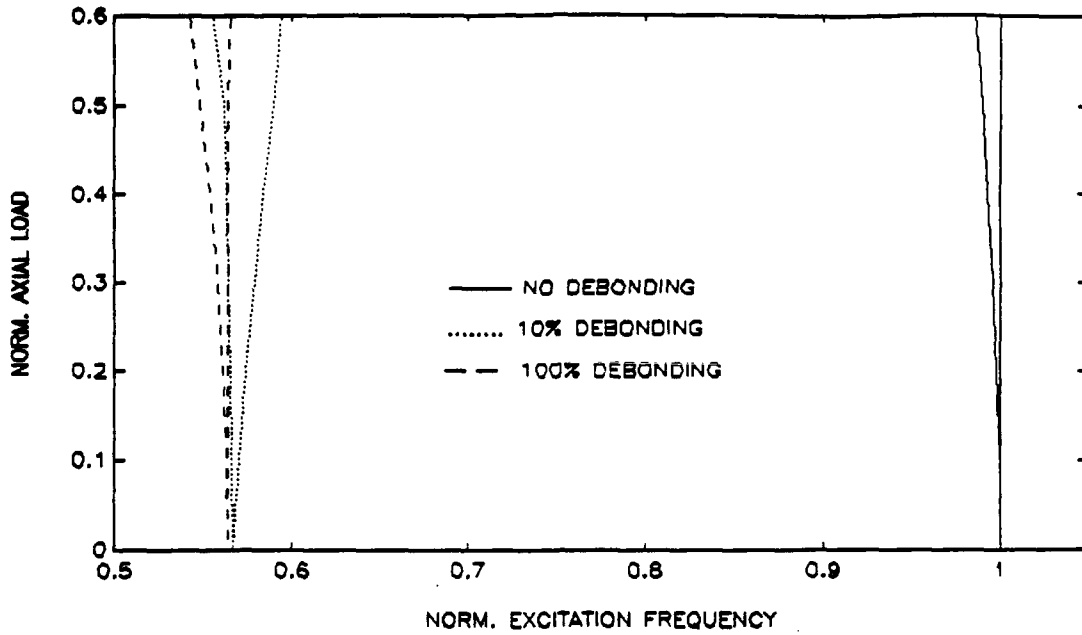


Figure 15. Instability domains boron-aluminum with free and simply supported ends (Dedonding started from the free end).

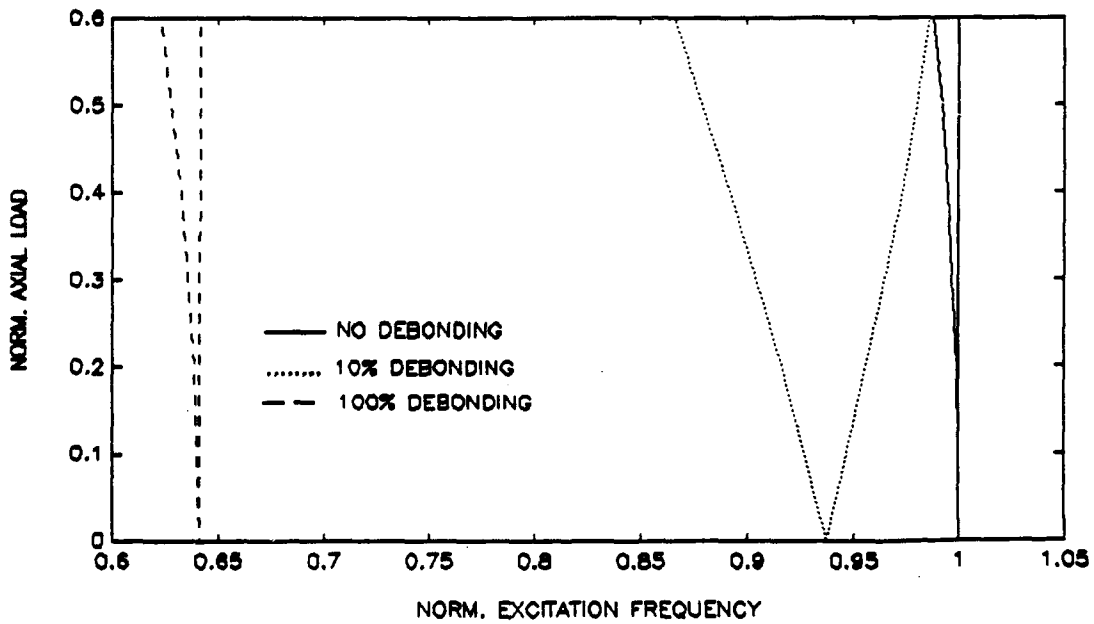


Figure 16. Instability domains graphite-epoxy with free and simply supported ends (Dedonding started from the simply supported end).

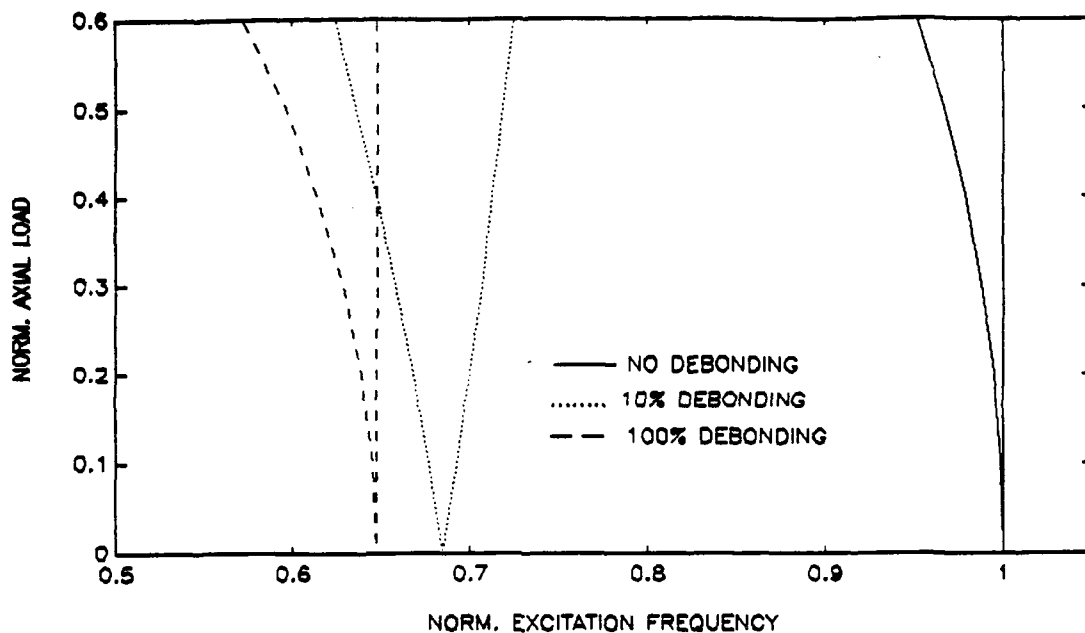


Figure 17. Instability domains of simply supported graphite-epoxy (Debonding started from the center).

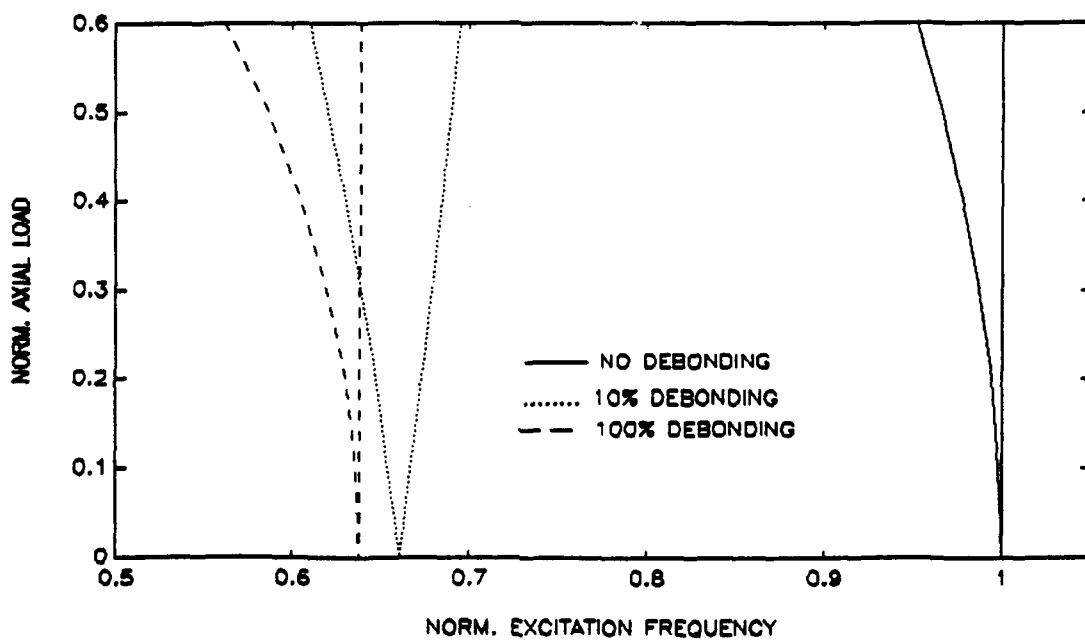


Figure 18. Instability domains of simply supported Kevlar-epoxy (Debonding started from the center).

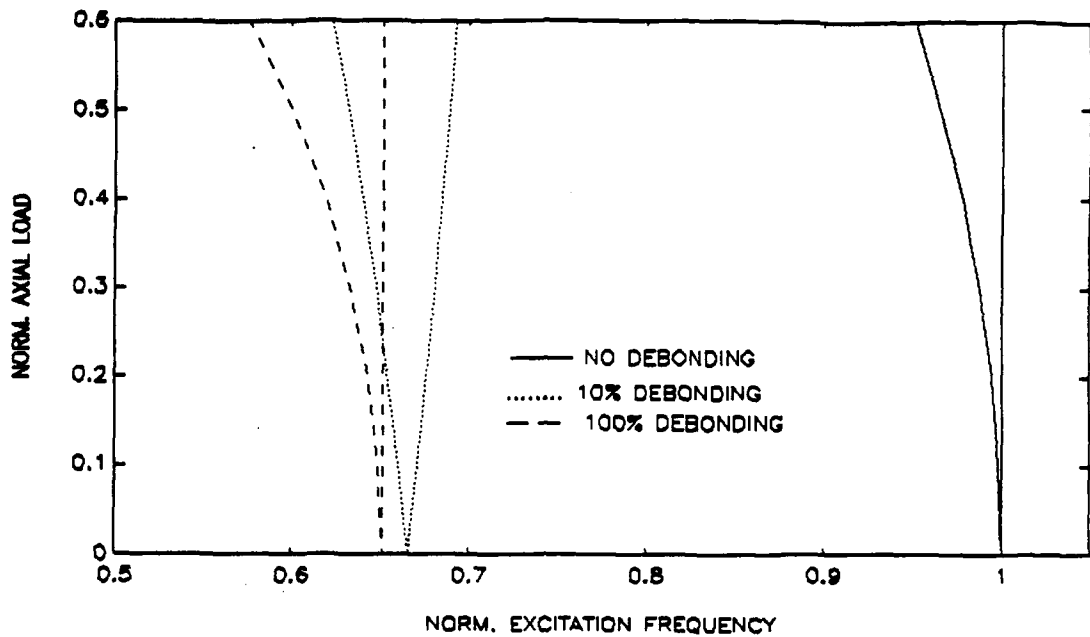


Figure 19. Instability domains of simply supported glass-epoxy (Dedonding started from the center).

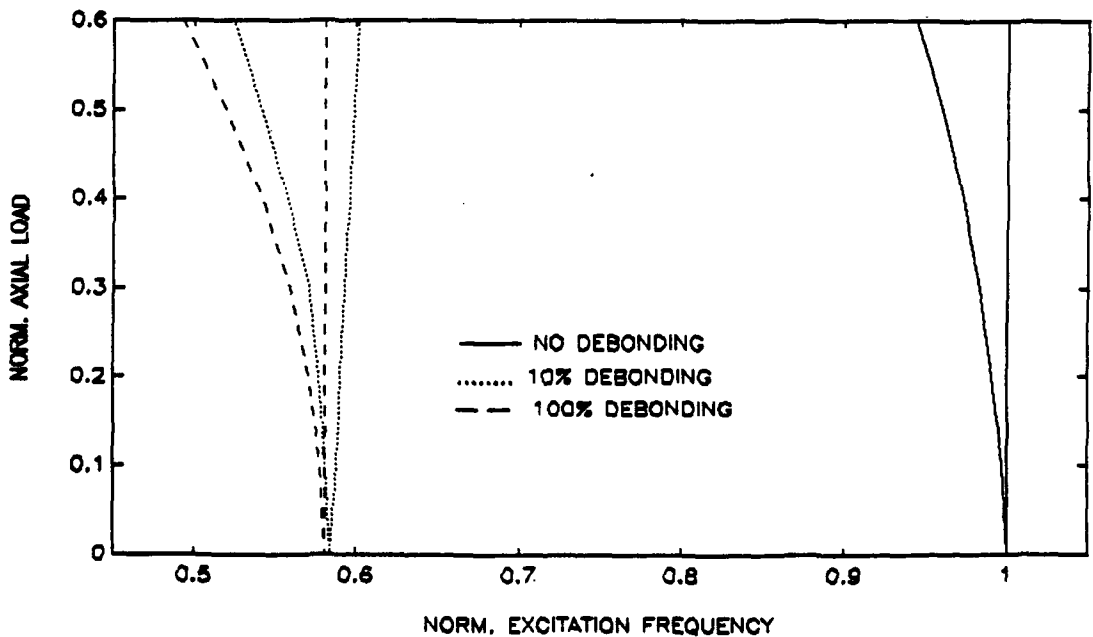


Figure 20. Instability domains of simply supported boron - aluminum (Dedonding started from the center).

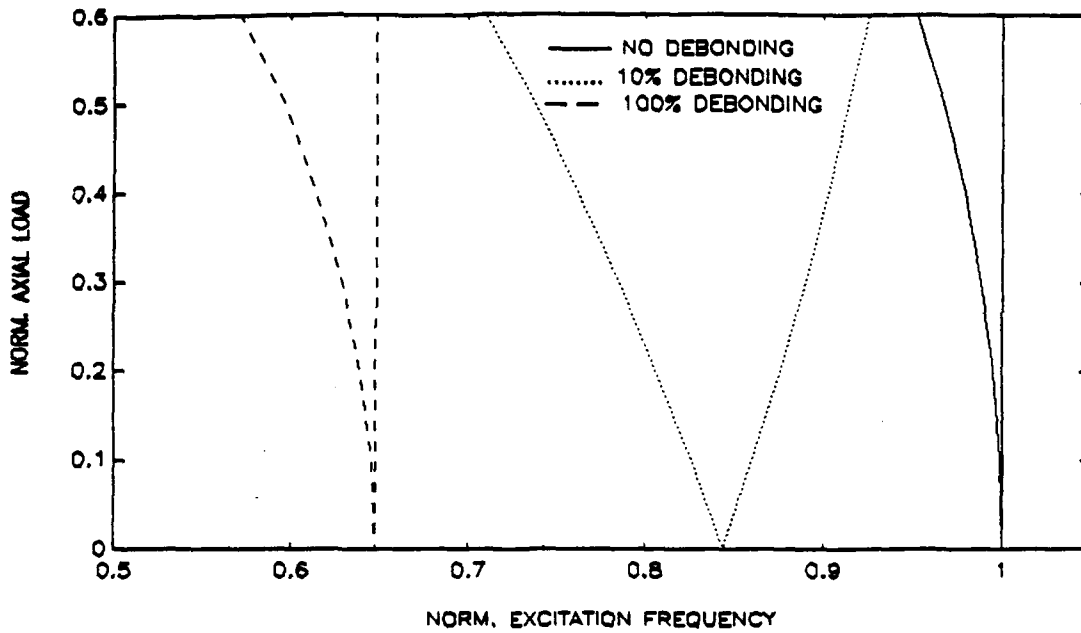


Figure 21. Instability domains of simply supported graphite-epoxy (Dedonding started from the ends).

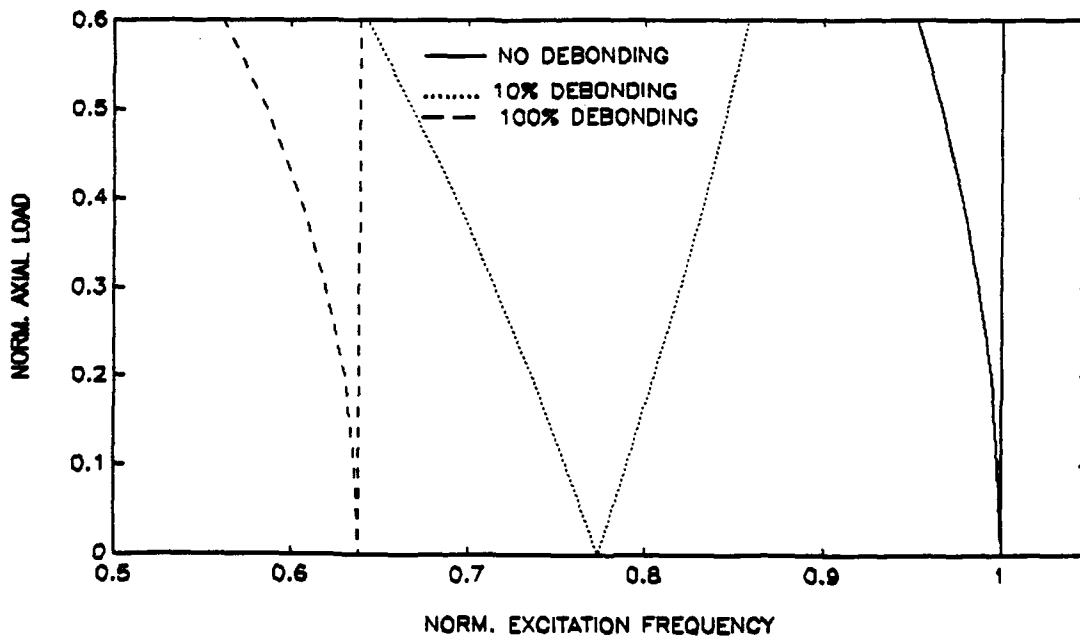


Figure 22. Instability domains of simply supported Kevlar-epoxy (Dedonding started from the ends).

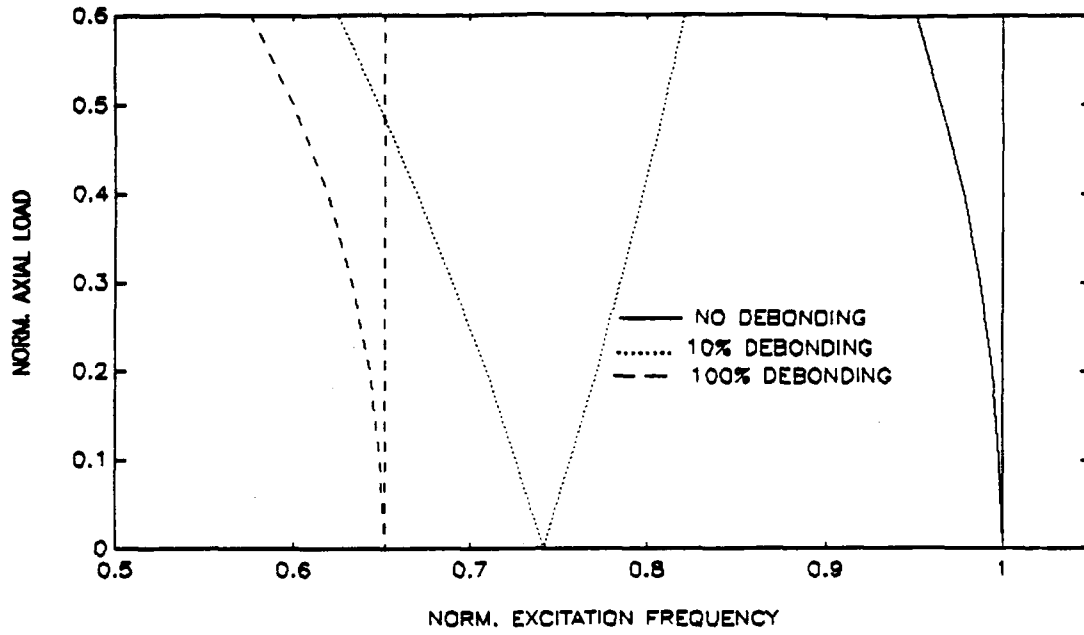


Figure 23. Instability domains of simply supported glass-epoxy (Dedonding started from the ends).

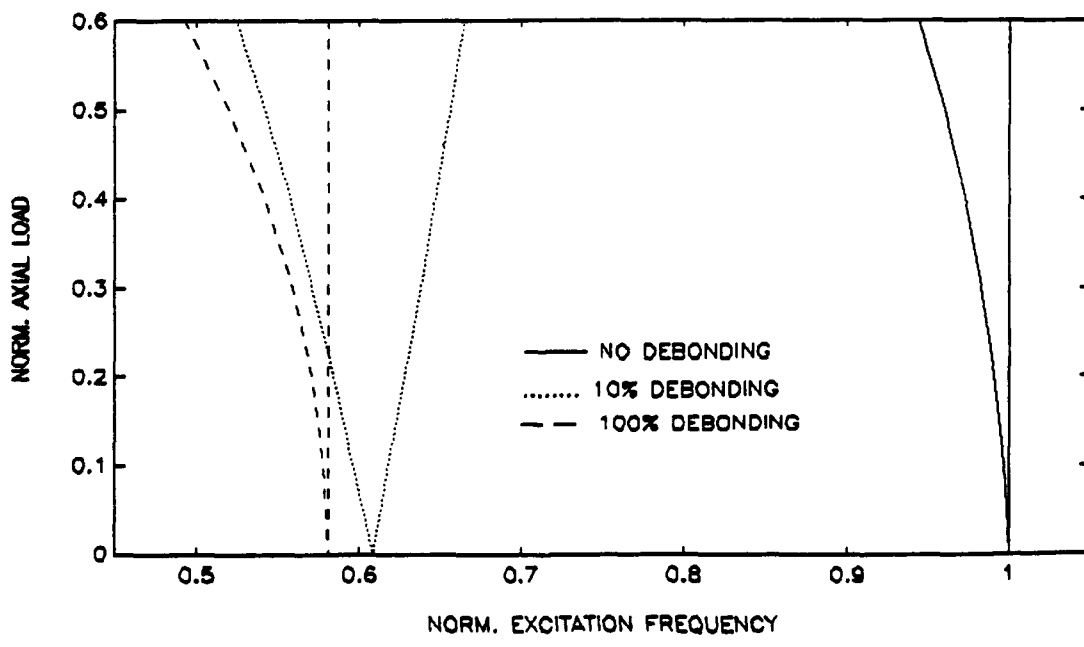


Figure 24. Instability domains of simply supported boron - aluminum (Dedonding started from the ends).

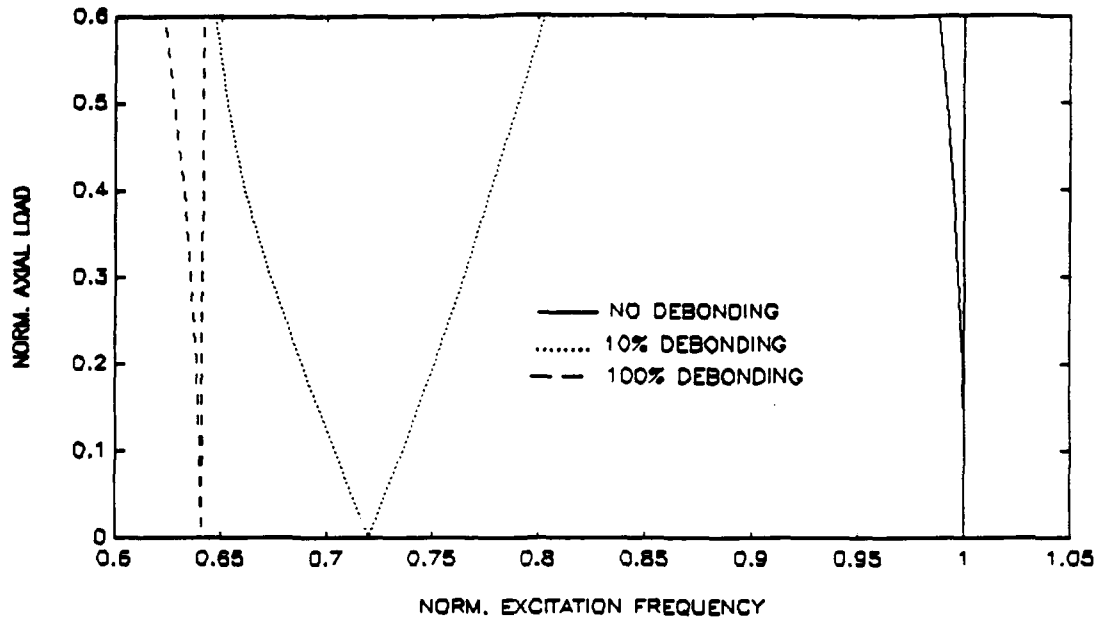


Figure 25. Instability domains graphite-epoxy with free and simply supported ends (Dedonding started from the free end).

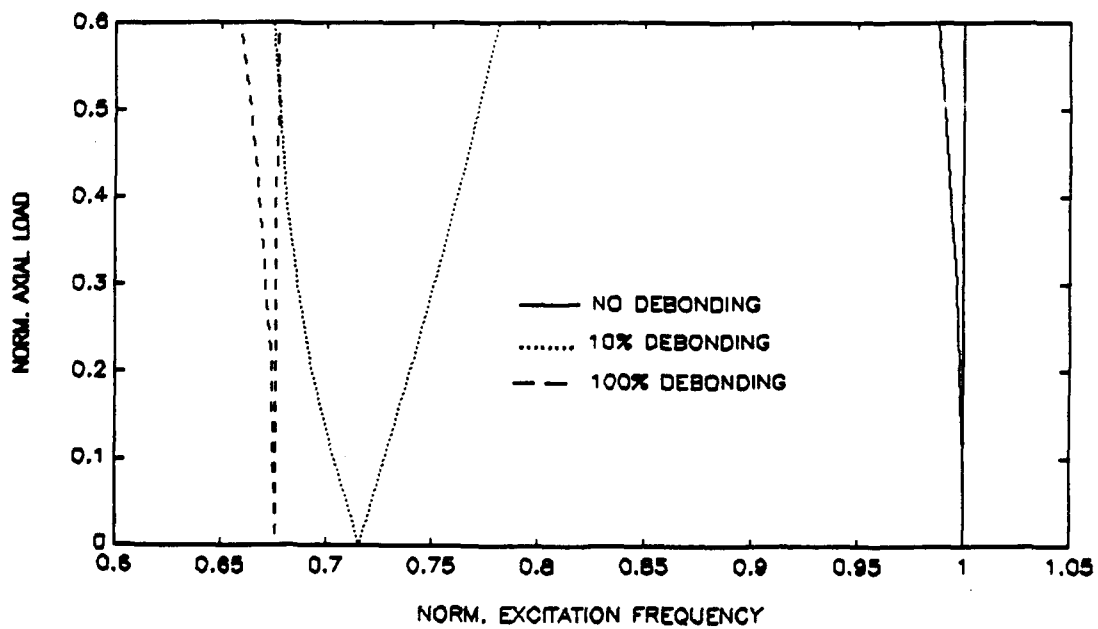


Figure 26. Instability domains Kevlar-epoxy with free and simply supported ends (Dedonding started from the free end).

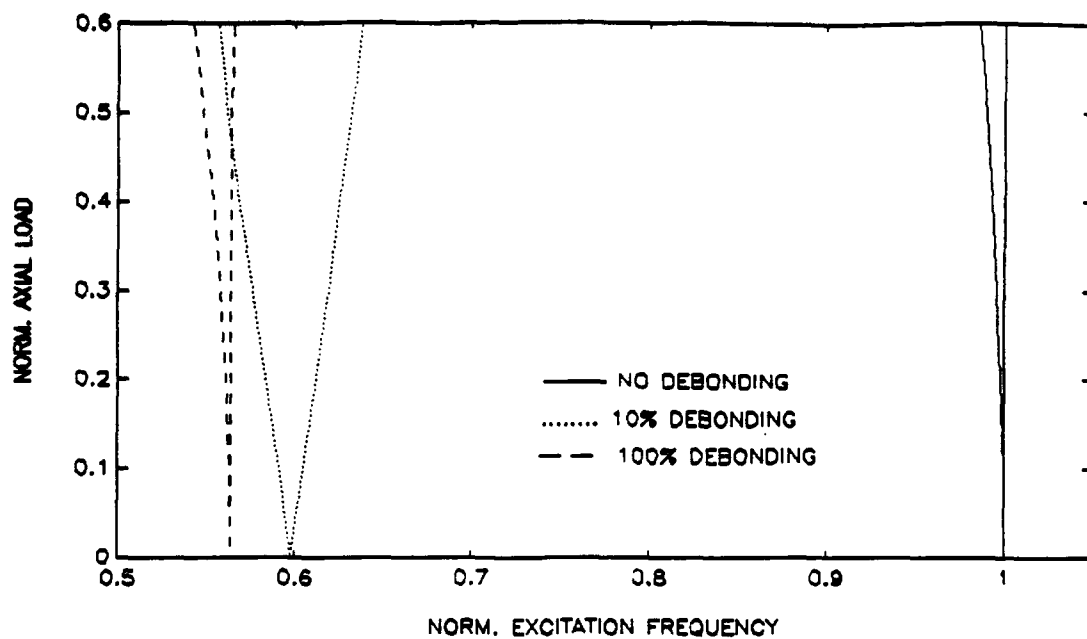


Figure 27. Instability domains boron-aluminum with free and simply supported ends (Debonding started from the simply supported end).

IV. CONCLUSIONS

An interfacial debonding between a fiber and a supporting matrix made a significant effect on the critical static buckling load of the fiber. An initial debonding of size 10 percent of the fiber length was most critical for a simply supported fiber regardless of its location. Three different fiber materials embedded in the same epoxy matrix yielded almost the same percentage reduction of the critical buckling load even if their absolute magnitudes of buckling loads were different. For a free-simply supported fiber, a local debonding located at the free end was most critical for the buckling load. Any size of debonding located at any other position did not influence the critical buckling load. In addition, a fiber breakage around the center of fiber along with a partial interfacial debonding reduced the buckling loads more significantly.

Interfacial debonding effects on dynamic instability of embedded fibers were generally more critical than those on static buckling loads. Debonding not only lowered instability domains but also widened the domains. Debonding effects were more significant for a free-simply supported fiber than for a fiber with both ends simply supported. A local debonding of size of 10 to 20 percent of the fiber length was most influential in affecting the domain of dynamic instability.

Debonding effects were not sensitive to changes in the location of debonding or boundary conditions of a fiber.

LIST OF REFERENCES

Dale, W. C. and Baer E., 1974, "Fiber-buckling in Composite Systems: a Model for the Ultrastructure of Uncalcified Collagen Tissues", J. Materials Science, Vol. 9, pp. 369-382.

Dow, N. J. and Gruntfest, I. J., 1960, "Determination of Most-needed, Potentially Possible Improvements in Materials for Ballistic and Space Vehicles", General Electric Company, Air Force Contract AF 04(647)-269.

Fred, N. and Kaminetsky, J., 1964, "The Influence of Material Variables on the Compressive Properties of Parallel Filament Reinforced Plastics", Proc. of 19th Annual Technical and Management Conf., Reinforced Plastics Division, Soc. of Plastic Industry, pp.(9-A)1-10.

Hahn, H. T. and Williams, J. G., 1984, "Composite Failure Mechanisms in Unidirectional Composites", NASA TM 85834.

Herrmann, L. R., Mason W. E., and Chan, S. T. K., 1967, "Response of Reinforcing Wires to Compressive States of Stress", J. Composite Materials, Vol. 1, pp. 212-226.

Hetenyi, M., 1974, Beams on Elastic Foundation, The University of Michigan Press, Ann Arbor, Michigan.

Kwon, Y. W., 1991, Finite Element Analysis of Dynamic Instability of Layered Composite Plates Using a High-order Bending Theory", Computers and Structures, Vol. 38, No. 1, pp. 57-62.

Lager, J. R. and June, R. R., 1969, "Compressive Strength of Boron-Epoxy Composites", J. Composite Materials, Vol. 3, pp. 48-56.

Lanir, Y. and Fung Y. C. B., 1972, "Fiber Composite Columns Under Compression", J. Composite Materials, Vol. 6, pp. 387-401.

Leventz, B., 1964, "Compressive Applications of Large Diameter Fiber Reinforced Plastics", Proc. of 19th Annual Technical and Management Conf., Reinforced Plastics Division, Soc. of Plastic Industry, pp.(14-D)1-18.

Maewal, A, 1981, "Postbuckling Behavior of a Periodically Laminated Medium in Compression", Int. J. Solids Structures, Vol. 17, pp. 335-344.

Rosen, B. W., 1965, "Mechanics of Composite Strengthening", Fiber Composite Materials, Amer. Soc. for Metals, pp. 37-75.

Timoshenko, S. P. and Gere, J. M., 1961, Theory of Elastic Stability, McGraw Hill Book Co., New York.

Tsai, S. W. and Hahn, H. T., 1980, Introduction to Composite Materials, Technomic Publ.

Wass, A. M., Babcock, C. D. Jr., and Knauss W. G., 1989, "A Mechanical Model for Elastic Fiber Microbuckling", Composite Material Technology 1989, ASME PD-Vol. 24, pp. 203-215.

INITIAL DISTRIBUTION LIST

	No. of Copies
1. Defense Technical Information Center Cameron Sitation Alexandria, Virginia 22304-6145	2
2. Library, Code 52 Naval Postgraduate School Monterey, California 93943	2
3. Deniz Harp Okulu Tuzla Istanbul, Turkey	2
4. Golcuk Tersanesi Komutanligi Golcuk Kocaeli, Turkey	2
5. Taskizak Tersanesi Komutanligi Kasimpasa Istanbul, Turkey	2
6. Deniz Kuvvetleri Komutanligi Personel Egitim Daire Baskanligi Bakanliklar Ankara, Turkey	1
7. Professor Y.W. Kwon, Code ME/Kw Department of Mecanical Engineering Naval Postgraduate School Monterey, California 93943	1
8. Department Chairman, Code ME/Kk Department of Mecanical Engineering Naval Postgraduate School Monterey, California 93943	1
9. Naval Engineering Curricular Office (Code 34) Naval Postgraduate School Monterey, CA 93943	1
10. Dr. Rambert F. Jones, Jr. Submarine Structures Division Code 172, Bldg. 19 Room A236B David Taylor Research Center Bethesda, Maryland 20084-5000	1